Bacterial Tubulins A and B Exhibit Polarized Growth, Mixed-Polarity Bundling, and Destabilization by GTP Hydrolysis

César Díaz-Celis,[a,b]* Viviana I. Risca,[c]* Felipe Hurtado,[a] Jessica K. Polka,[d]*
Scott D. Hansen,[d]* Daniel Maturana,[a] Rosalba Lagos,[a] R. Dyche Mullins,[d]
Octavio Monasterio[a]

Laboratorio de Biología Estructural y Molecular, Departamento de Biología, Facultad de Ciencias, Universidad de Chile, Santiago, Chile[a]; Programa de Doctorado en Microbiología, Facultad de Química y Biología, Universidad de Santiago de Chile, Santiago, Chile[b]; Biophysics Graduate Group, University of California, Berkeley, California, USA[c]; Department of Cellular and Molecular Pharmacology, University of California, San Francisco, California, USA[d]

ABSTRACT Bacteria of the genus *Prosthecobacter* express homologs of eukaryotic α- and β-tubulin, called BtubA and BtubB (BtubA/B), that have been observed to assemble into filaments in the presence of GTP. BtubA/B polymers are proposed to be composed *in vitro* by two to six protofilaments in contrast to that *in vivo*, where they have been reported to form 5-protofilament tubes named bacterial microtubules (bMTs). The *btubAB* genes likely entered the *Prosthecobacter* lineage via horizontal gene transfer and may be derived from an early ancestor of the modern eukaryotic microtubule (MT). Previous biochemical studies revealed that BtubA/B polymerization is reversible and that BtubA/B folding does not require chaperones. To better understand BtubA/B filament behavior and gain insight into the evolution of microtubule dynamics, we characterized *in vitro* BtubA/B assembly using a combination of polymerization kinetics assays and microscopy. Like eukaryotic microtubules, BtubA/B filaments exhibit polarized growth with different assembly rates at each end. GTP hydrolysis stimulated by BtubA/B polymerization drives a stochastic mechanism of filament disassembly that occurs via polymer breakage and/or fast continuous depolymerization. We also observed treadmilling (continuous addition and loss of subunits at opposite ends) of BtubA/B filament fragments. Unlike MTs, polymerization of BtubA/B requires KCl, which reduces the critical concentration for BtubA/B assembly and induces it to form stable mixed-orientation bundles in the absence of any additional BtubA/B-binding proteins. The complex dynamics that we observe in stabilized and unstabilized BtubA/B filaments may reflect common properties of an ancestral eukaryotic tubulin polymer.

IMPORTANCE Microtubules are polymers within all eukaryotic cells that perform critical functions; they segregate chromosomes, organize intracellular transport, and support the flagella. These functions rely on the remarkable range of tunable dynamic behaviors of microtubules. Bacterial tubulin A and B (BtubA/B) are evolutionarily related proteins that form polymers. They are proposed to be evolved from the ancestral eukaryotic tubulin, a missing link in microtubule evolution. Using microscopy and biochemical approaches to characterize BtubA/B assembly *in vitro*, we observed that they exhibit complex and structurally polarized dynamic behavior like eukaryotic microtubules but differ in how they self-associate into bundles and how this bundling affects their stability. Our results demonstrate the diversity of mechanisms through which tubulin homologs promote filament dynamics and monomer turnover.

Address correspondence to César Díaz-Celis, cesardiazcelis@gmail.com, or Octavio Monasterio, monaster@uchile.cl.

* Present address: César Díaz-Celis, Howard Hughes Medical Institute, University of California, Berkeley, California, USA; Viviana I. Risca, Department of Genetics, Stanford University School of Medicine, Stanford, California, USA; Jessica K. Polka, Whitehead Institute, Cambridge, Massachusetts, USA; Scott D. Hansen, California Institute for Quantitative Biosciences, University of California, Berkeley, California, USA.

C.D.-C. and V.I.R. contributed equally to this article.

Bacterial tubulin A and bacterial tubulin B (BtubA/B) are the closest known bacterial homologs of eukaryotic tubulin ($\sim$35% sequence identity with α- and β-tubulin) (1). They interact to form the BtubA/B heterodimer that polymerizes in the presence of GTP (2, 3). *btubA* and *btubB* genes were discovered, along with a kinesin light chain homolog (*bklc*), in the genomes of four *Prosthecobacter* bacterial species (1) to form the bacterial tubulin operon (*btub* operon) (4). Because of this high sequence identity and structural similarity, it has been proposed that *Prosthecobacter* acquired the *btub* operon by horizontal gene transfer (1–7) from an unknown species. Although the function of BtubA/B in *Prosthecobacter* remains unknown, they may contribute to the elongated shape of the *Prosthecobacter* cell (2) or serve as a scaffold for the formation of the cell stalk (5).

BtubA/B polymer structure is not yet well established, and several filament structures have been observed *in vivo* and *in vitro*. BtubA/B filaments observed *in vivo* in several species of *Prosthecobacter* using cryoelectron tomography have been proposed to consist of 7.6-nm-wide hollow tubes formed by 5 protofilaments (8). This structure was named a bacterial microtubule (bMT), and it has been suggested that it represents the ancient precursor of eukaryotic microtubules (8). However, single BtubA/B filaments formed *in vitro* and observed using negative stain electron microscopy (EM) have been interpreted to consist of two parallel protofilaments (2, 3), although some filament bundles have appeared to form a lumen (2). Observations with cryoelectron microscopy of *in vitro* assembled filaments are also consistent with helical polymers composed of 2 to 6 protofilaments (9). Based on results of pelleting assays (2, 3) and mutagenesis studies (10), it has been inferred that BtubA/B protofilaments contain a polar, alternating linear arrangement of BtubA/B heterodimers. By comparison, eukaryotic MTs are tubular, 25-nm-wide polymers formed *in vivo* by 13 protofilaments, each of which is a polar chain of α/β-tubulin heterodimers (11). MTs are also kinetically polar, with different assembly/disassembly rates at the two ends (12, 13). Polymerization studies have not yet established whether the two ends of BtubA/B filaments polymerize at different rates.

The eukaryotic tubulins, α/β-tubulin; the better-characterized bacterial tubulins, FtsZ and TubZ; and the newly discovered bacteriophage tubulin, PhuZ, are assembly dependent GTPases that polymerize when GTP bound and are destabilized by hydrolysis of GTP to GDP (14, 15). Similar to α/β-tubulin and FtsZ assembly, BtubA/B polymerization is GTP dependent, cooperative, and reversible, and GTP hydrolysis is coupled to assembly (2, 3, 5). Structural changes in the polymer associated with GTP hydrolysis give rise to complex behaviors in the tubulin family, including dynamic instability observed in eukaryotic MTs (stochastic transitions between growing and shortening phases at microtubule ends [11, 12, 16]) and treadmilling observed in several types of tubulin family polymers (concomitant assembly at one end and disassembly at the other [11]). Whether BtubA/B filaments exhibit any of these or other dynamic behaviors remains an open question.

In order to obtain insight into the dynamics and polarity of BtubA/B polymers, we characterized their assembly *in vitro* with confocal fluorescence microscopy, electron microscopy, light scattering, high-speed pelleting, and GTPase assays. We determined that, like eukaryotic MTs, BtubA/B filaments polymerized *in vitro* are kinetically polar polymers that are destabilized by GTP hydrolysis. They exhibit stochastic growth and disassembly and treadmilling. Salt stimulates BtubA/B polymerization by reducing the critical concentration for assembly. Unlike eukaryotic MTs, BtubA/B filaments form stable apolar bundles at medium to high potassium concentrations without any bundling or stabilizing microtubule-binding proteins.
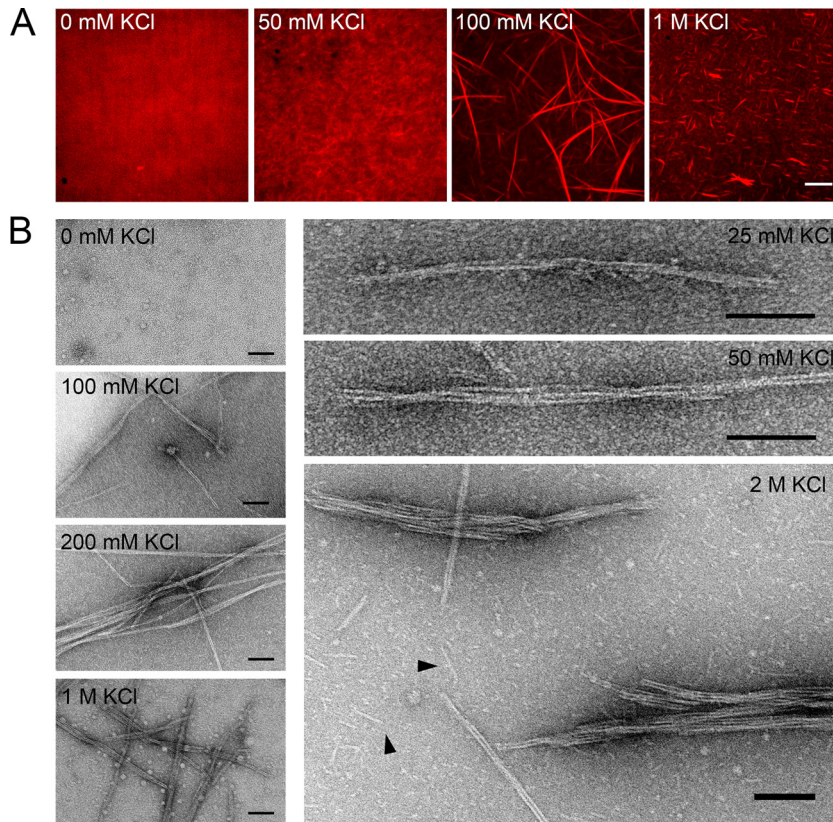
FIG 1 BtubA/B filament morphology and KCl-dependent bundling. (A) A total of 5 μM BtubA/B (15% TAMRA labeled) was polymerized with 1 mM GTP in polymerization buffer (50 mM HEPES-KOH [pH 7], 5 mM MgCl$_2$) with various KCl concentrations. After 5 min, the samples were applied to a poly-L-lysine-coated coverslip and visualized by confocal microscopy. (B) A total of 5 μM BtubA/B was polymerized with 1 mM GTP for 5 min at room temperature in various KCl concentrations. BtubA/B filaments were stained with uranyl formate 0.75% for EM. BtubA/B filaments were not observed at 0 M KCl. Above 50 mM KCl, filaments associated to form bundles. At 2 M KCl, bundles coexist with single BtubA/B filaments and small structures (arrowheads). (A) Scale bar, 10 μm; (B) scale bars, 100 nm.

RESULTS

Potassium induces BtubA/B assembly and bundling. We designed a new purification method for untagged recombinant BtubA/B based on the standard α/β-tubulin method of successive cycles of polymerization-depolymerization (see Fig. S1 in the supplemental material) in the presence of MgCl$_2$ and KCl, which are known to be necessary for polymerization (3, 5). Interestingly, it was not possible to purify BtubA/B using NaCl instead of KCl, and increasing the KCl concentration increased the yield. This suggested to us that potassium regulates a yet uncharacterized BtubA/B assembly parameter.

To determine the effect of KCl on BtubA/B polymer assembly, we used confocal microscopy to visualize GTP-induced polymerization of fluorescently labeled BtubA/B (Fig. 1A). In the absence of KCl, we did not observe discernible filamentous structures. Short and dispersed BtubA/B filaments are visible at 50 mM KCl, and a network of BtubA/B filament bundles appears at 100 mM KCl. At 1 M KCl, bundles increase in number but decrease in length, preventing the formation of a network of bundles. The observed decrease in bundle length is likely due to the large number of BtubA/B filament ends, which quickly use up the protein available for BtubA/B filament elongation.

Using negative stain EM, we observed at 25 mM KCl what appeared to be a single filament composed of a pair of BtubA/B protofilaments with a narrow dark space between them (Fig. 1B), which is consistent with a filament formed by paired proto-

filaments as previously observed *in vitro* (2, 3). At 50 mM KCl, we observed that BtubA/B filaments interact, forming bundles composed of a few BtubA/B filaments. Bundling observable by EM at higher salt concentrations was consistent with fluorescence microscopy results (Fig. 1A). At 100 and 200 mM KCl, we observed multiple paired protofilaments forming long bundles. BtubA/B bundles decrease in length at 1 M KCl. At 2 M KCl, we also observed short linear structures, smaller than a single BtubA/B filament, which were not visible below 200 mM KCl (Fig. 1B).

We characterized the effect of potassium on BtubA/B assembly kinetics by 90° light scattering (see Fig. S2 in the supplemental material) and observed sigmoidal kinetic traces below 25 mM KCl and nonsigmoidal light scattering signal trajectories at KCl concentrations at which we observe filament bundling by microscopy (Fig. 1; see also Fig. S2).

We observed that the protein concentration at which BtubA/B assembly was first detected decreases with increasing KCl, a trend observed over all KCl concentrations employed. This suggests that KCl affects not only BtubA/B filament bundling but also filament formation. Because light scattering is proportional to the amount of assembled polymer and its spatial organization (17), we determined the critical concentration of BtubA/B assembly from the plot of the maximum scattering intensity versus BtubA/B concentration (Fig. 2A) (13, 18). However, we only used data between 0 and 25 mM KCl to avoid the confounding effects of bundling. From the x axis intersections of Fig. 2A, we determined that, in the absence of KCl, the critical concentration for BtubA/B assembly is 9.5 μM, and it decreases to 3.8 μM at 25 mM KCl (see Table S1 in the supplemental material). The lack of assembled BtubA/B filaments at 0 mM KCl (Fig. S2A) and visualized by EM (Fig. 1B) is explained because EM experiments were done using 5 μM BtubA/B, which is below the critical concentration for assembly.

To determine whether KCl has an effect on BtubA/B nucleation in this low-salt regime, we normalized the log of the maximum rate of assembly (V_{max}) by the maximum intensity (I_{max}) of each polymerization trace, and this value was plotted versus the log of the BtubA/B available to polymerize (total BtubA/B minus critical concentration of BtubA/B assembly) (Fig. 2B). The slope of the linear fit is equivalent to half of the nucleus size ($n/2$) (19) and suggests that the rise of KCl concentration increased the size of the BtubA/B polymerization nucleus. At 0 mM KCl, the slope of the linear fit is ~0.3, suggesting that the nucleus consists of just a monomer (BtubA or BtubB). At 3.1 mM KCl, the nucleus is composed of one BtubA/B heterodimer ($n/2 = $ ~0.5), and at 12.5 to 25 mM KCl, the slope of the linear fit ($n/2 = $ ~1) suggests that the nucleus is composed of two BtubA/B heterodimers.

As an independent measurement, we determined the amount of assembled BtubA/B polymers and the critical concentration of BtubA/B assembly as a function of KCl concentration using high-speed pelleting. The increase from 0 to 2 M KCl produced an increase in the mass of assembled polymer (Fig. 2C) and reduced the critical concentration for BtubA/B assembly (Fig. 2D; Table S1). To deconvolve the effects of KCl and polymer concentration on bundling, we compared BtubA/B assembly kinetics under conditions that produce a similar mass of polymers (20) (Fig. 2E). Polymerization curves show that at a similar polymer concentration, the increase in KCl concentration increases the light scattering intensity, indicating that filament bundling is influenced by salt concentration in addition to filament concentration.

Effect of KCl on GTPase activity of BtubA/B. Because the dynamic assembly and disassembly of eukaryotic microtubules and bacterial FtsZ filaments are regulated by GTP binding, hydrolysis, and exchange, we analyzed BtubA/B GTPase activity at different KCl concentrations (Fig. 2F; Table S1). In the absence of KCl, the GTPase activity was 0.96 ± 0.03 mol GTP per minute per mole of BtubA/B, which increased slightly to 1.36 ± 0.11 mol GTP per minute per mole of BtubA/B at 25 mM KCl. However, at KCl concentrations above 50 mM, the GTPase activity decreased continuously to 0.3 ± 0.02 mol GTP per minute per mole of BtubA/B in 2 M KCl.

Polymerization of BtubA/B filaments is kinetically polarized at low and intermediate salt concentrations. Like eukaryotic microtubules, the BtubA/B polymer is
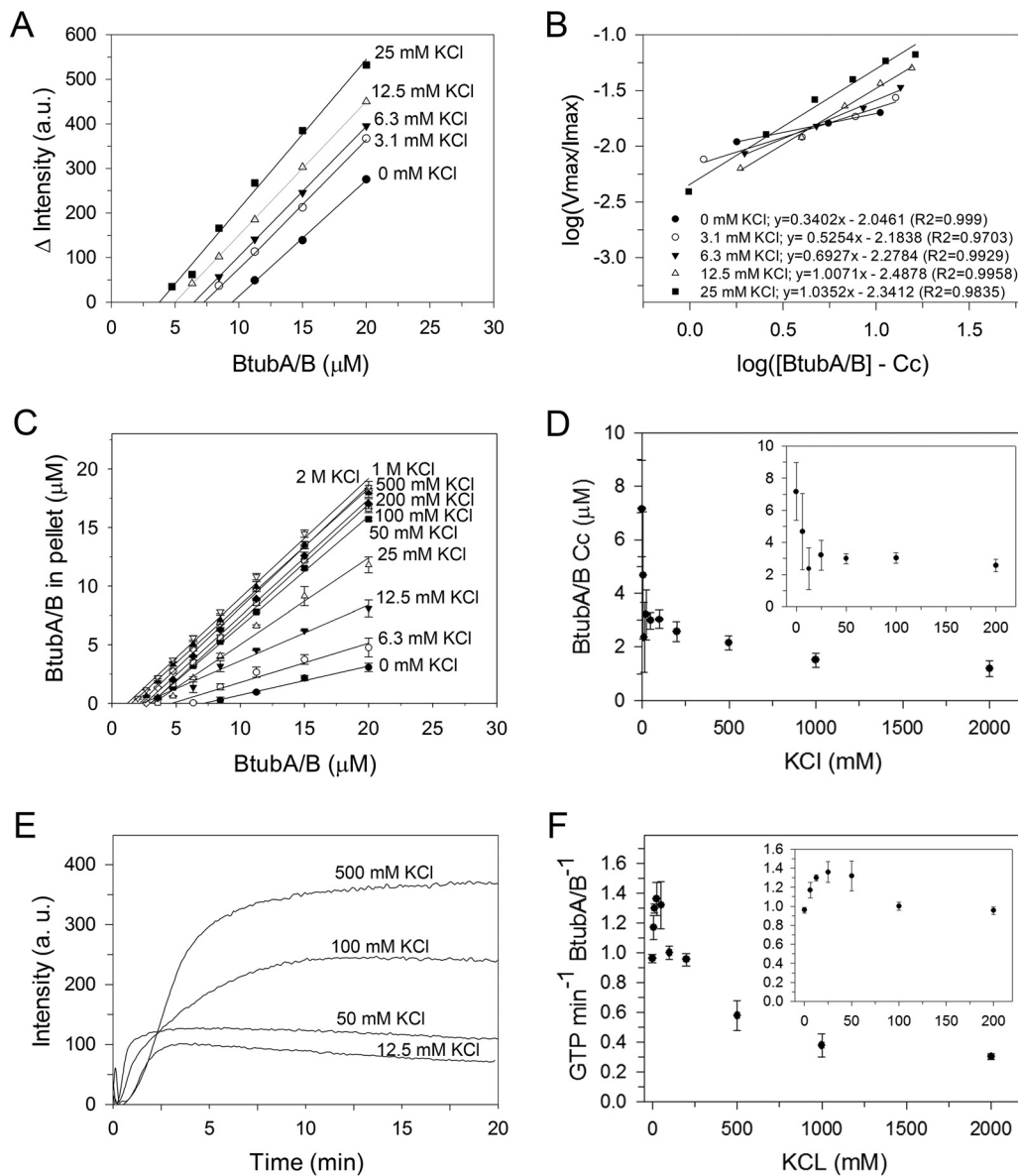
FIG 2 The increase of KCl reduces the critical concentration, increases the mass of assembled BtubA/B filaments, and reduces GTP hydrolysis. Light scattering, high-speed pelleting, and GTPase activity of BtubA/B polymerization. (A) Estimation of the critical concentration of BtubA/B polymerization below 25 mM KCl. The maximum light scattering intensity from each polymerization time course under each condition (see Fig. S2 in the supplemental material) is plotted versus the initial BtubA/B concentration. The x-intercept of each linear fit corresponds to the critical concentration. (B) Determination of the polymer nucleus size between 0 and 25 mM KCl shows that the rise of KCl concentration increased the size of the polymerization nucleus. The log of the maximum rate of assembly (V_{max}) at each KCl condition was normalized by the maximum intensity (I_{max}) and was plotted versus the log of the BtubA/B available to polymerize (total BtubA/B minus critical concentration). The slope of the linear fit corresponds to half of the nucleus size (n/2) (19). The inset shows the linear fit equation, where "x" corresponds to the slope and "R2" corresponds to the R-squared value. (C) Different BtubA/B concentrations were polymerized at different KCl concentrations by addition of 1 mM GTP and centrifuged at 25°C at 100,000 × g. The amount of BtubA/B pelleted was plotted against total BtubA/B concentration. The x-intercept of the linear fit corresponds to the BtubA/B critical concentration. (D) Critical concentration of BtubA/B polymerization determined by high-speed pelleting versus KCl concentration. The inset corresponds to an expanded view at lower KCl concentrations. (E) Comparison of four BtubA/B light scattering polymerization curves (data from Fig. S2 in the supplemental material) based on the BtubA/B polymer concentration determined by high-speed pelleting (Fig. 2C). Polymerization conditions were 8.4 μM BtubA/B in 12.5 mM KCl (3.2 μM BtubA/B polymer), 6.3 μM BtubA/B in 50 mM KCl (3.2 μM BtubA/B polymer), 4.7 μM BtubA/B in 100 mM KCl (1.6 μM BtubA/B polymer), and 3.6 μM BtubA/B in 500 mM KCl (1.3 μM BtubA/B polymer). Polymerization kinetics in 12.5 mM KCl exhibited sigmoidal behavior and the lowest maximum intensity between the conditions. However, increasing KCl to 50 mM KCl increased the light scattering intensity. The increase in signal intensity was greater in the transition to 100 mM KCl, where the trace exhibited an elongation phase composed of two steps as described for Fig. S2G. At 500 mM KCl, two steps cannot be resolved in the elongation phase, and depolymerization is slower. (F) GTPase activity of BtubA/B versus KCl concentration. The inset shows the expanded view of GTPase activity at low salt.
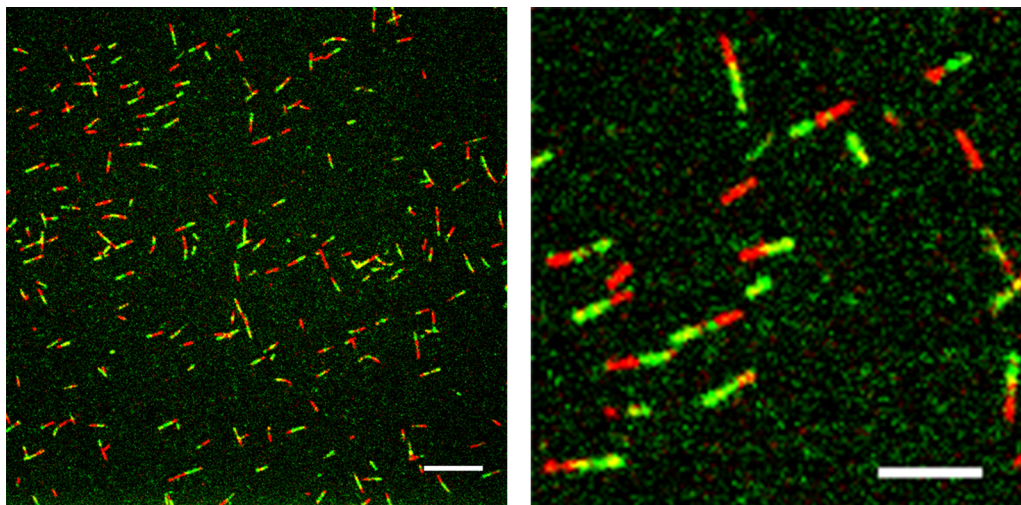
FIG 3 BtubA/B filament assembly is kinetically polar at low salt. Kinetic polarity assay of BtubA/B (see Materials and Methods). TAMRA-labeled BtubA/B (red) was polymerized with 0.5 mM GMPCPP in 25 mM KCl. After 2 min, Alexa Fluor 488-labeled BtubA/B (green) was added. Right image corresponds to a magnification of the left image. Scale bars, 10 μm in left image and 5 μm in right image.

thought to be structurally polar (10), but this does not necessarily imply that the kinetics of assembly are also polar. For example, the structurally polar actin homolog ParM (21) elongates symmetrically (22, 23). To test the hypothesis that BtubA/B filaments exhibit kinetic polarity, we studied their assembly by fluorescent filament imaging (22) using BtubA/B seeds labeled with 5 (and 6)-carboxytetramethylrhodamine, succinimidyl ester (TAMRA) (red) and soluble BtubA/B labeled with Alexa Fluor 488 (green) at a low salt concentration to avoid the confounding effects of bundling. Most of the observed filaments (90%) had one red end and one green end (Fig. 3), indicating that, as for eukaryotic microtubules, the growth of BtubA/B filaments is kinetically polar. Polar filaments were clearly observed from 12.5 mM KCl up to 100 mM KCl (see Fig. S3 in the supplemental material). At higher KCl concentrations, we observed thicker yellow polymers, which we interpret as mixed-polarity bundles of BtubA/B filaments. Following eukaryotic microtubule nomenclature, we refer to the fast-growing end as the filament's plus end (+) and to the slow-growing end as its minus end (−).

BtubA/B bundle and filament assembly at intermediate salt concentration. To gain insights into BtubA/B assembly dynamics, we monitored the assembly dynamics of fluorescently labeled BtubA/B filaments growing from seeds stabilized with GMPCPP (guanylyl 5'-α,β-methylenediphosphonate; a slowly hydrolyzable GTP analogue) at 100 mM KCl using confocal fluorescence microscopy. We determined that BtubA/B labeled with TAMRA show an increased critical concentration for assembly (7.3 μM BtubA/B) compared to that of the unlabeled protein (4.9 μM BtubA/B) (see Fig. S4A in the supplemental material), but this critical concentration increase is within the range of values that we observe for experimental conditions at different salt concentrations (see Table S1). We therefore expect that the BtubA/B filament properties that we observe will be modestly perturbed but qualitatively consistent with the behavior of the unlabeled polymer. Consistent with our bulk polymerization results, 3 μM BtubA/B in 100 mM KCl and GTP, filaments growing at 3.7 $\pm$ 0.2 μm min^{-1} ($n = 8$) formed long and interconnected bundles (Fig. 4A; see also Movie S1 in the supplemental material). BtubA/B filament bundling occurs through the interaction of parallel or antiparallel individual growing filaments, forming thin bundles, which in turn interact together (zippering) to form thicker and longer bundles (as observed by an increase in fluorescence intensity) (Fig. 4B and C; Movie S1). Some GMPCPP-stabilized BtubA/B filament seeds also elongated as a bipolar bundle (Fig. 4A; Movie S1), confirming that bundles are composed of mixed-polarity filaments.
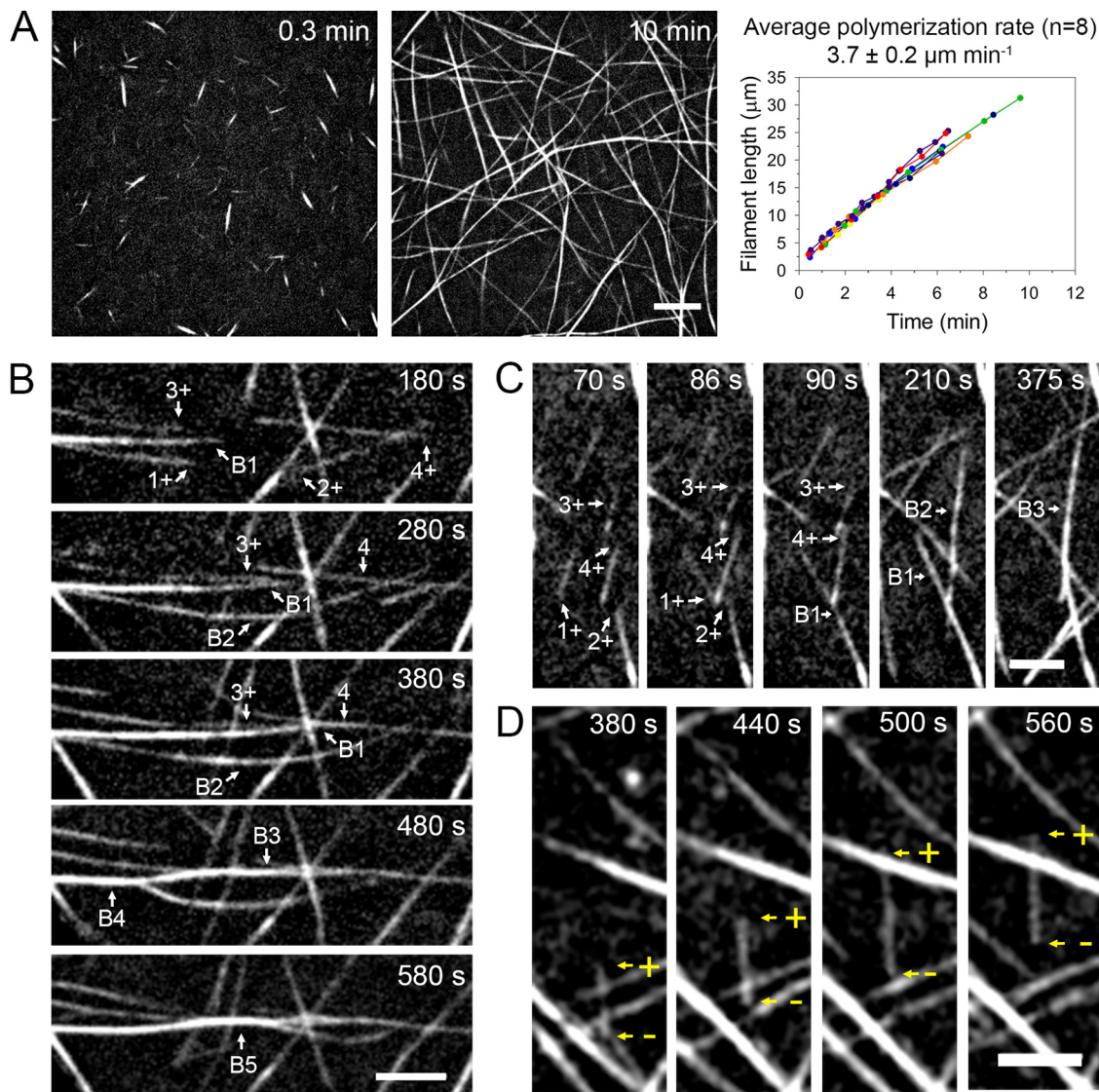
FIG 4 Visualization of BtubA/B polymerization and filament bundling at intermediate KCl concentration. (A) Time course of BtubA/B polymerization (3 μM BtubA/B, 30% TAMRA labeled) from GMPCPP-stabilized seeds (brighter labeling) in 50 mM HEPES (pH 7), 5 mM MgCl$_2$, 100 mM KCl, and 1 mM GTP. (Right) Filament length versus time for eight individual filaments. (B) Two filaments growing in opposite directions ("1" and "2," where + denotes the growing end of the filament) interact end to end, forming a bundle (B2). Two single BtubA/B filaments ("3+" and "4+") and a bundle (B1) interact longitudinally to form a thicker bundle (B3). At 480 s and 580 s, bundles B2 and B3 zipper together (B4 and B5). (C) Dynamics of BtubA/B bundles formed by parallel and antiparallel filament annealing. A bundle (B1) formed by the interaction of two antiparallel growing BtubA/B filaments ("1+" and "2+") interacts with a bundle (B2) formed by two parallel growing BtubA/B filaments ("3+" and "4+"), forming bundle B3. (D) Filament treadmilling. The rate of polymerization of the BtubA/B filament growing end ("+") is similar to the depolymerization rate at the other end ("−"). Images were preprocessed as described in Materials and Methods. Scale bars, 10 μm (A) and 5 μm (B to D).

Interestingly, we observed BtubA/B filament treadmilling, consisting of simultaneous growth at the plus end and subunit loss at the minus end (Fig. 4D; Movie S1), in fragments whose minus ends were not stabilized by a seed. These fragments indicate that breakage events do occur under these conditions and that the critical concentration must be different between their plus and minus ends. Although it is possible that apparent treadmilling is also due to unidirectional filament sliding along its length while the filament is also growing, the purity of our BtubA/B purification (Fig. S1) makes motor-based sliding unlikely.

BtubA/B filaments in low salt exhibit steady growth punctuated by stochastic shortening. In order to explore the dynamics of single filaments in more detail without the confounding effects of bundling, we visualized the assembly of 30% labeled, 3 μM

TAMRA-labeled BtubA/B in 12.5 mM KCl and GTP (Fig. 5A; see also Movie S2 in the supplemental material). In the vast majority of cases, we observed filaments with similar cross-sectional fluorescence profiles and strength of thermal bending fluctuations growing from seeds in one direction, which we interpret as single filaments (Fig. S4B and C). Rarely, we observed brighter and stiffer filaments whose fluorescence was a factor of 2 or 4 brighter than single filaments and whose ends could be seen to occasionally fray into fluctuating single filaments. We interpreted these as thin bundles. We also observed two or more filaments growing from seeds in opposite directions. The average rate of filament growth was 2.4 ± 0.3 μm min^{-1} ($n = 7$).

We observed that BtubA/B filaments stochastically switch from steady growth to a shortening phase (Fig. 5A; Movie S2). Some filaments shortened down to the seed end, while other filaments partially reduced in length. In both cases, the elongation phase from the plus end resumed at a similar rate as before. The elongation time until the first shortening event varied among the filaments, indicating stochastic switching between elongation and shortening (22). Shortening appears to be due to breakage of a fragment from the growing tip (Fig. 5B; see also Movie S3 in the supplemental material) and/or extremely fast depolymerization (Fig. 5C; Movie S3). Although fluctuating filament ends did not always make it possible to measure filament length at every frame, we were able to estimate the instantaneous shrinkage rate to have a distribution with approximately two sets of values, a low depolymerization rate with an average of 32 μm min^{-1} and a high set of rates with an average of 175 μm min^{-1} (Fig. 5E). It is possible that the fast depolymerization population involves fragmentation of BtubA/B filaments, creating short fragments that diffuse away or depolymerize from their unstabilized minus end too quickly to be observed (Fig. 5B). However, we also occasionally observed filament fragments bound to the surface after breakage, which depolymerized from their new minus ends at a higher rate than the growing plus ends, causing the disassembly of the filament fragment (Fig. 5D; Movie S3). As expected, the increase of the BtubA/B concentration from 3 μM to 5 μM produced longer and faster-growing filaments (see Fig. S4D and Movie S4 in the supplemental material) and also increased the lifetime of BtubA/B filament fragments without stabilized minus ends (Fig. S4E and Movie S4). We also observed filament shortening caused by a growing filament end running into a perpendicularly aligned filament (Fig. S4F and Movie S4).

The dynamic instability model of eukaryotic microtubules predicts that the stochastic shrinkage is dependent on GTP hydrolysis in the MT wall (11–13, 16). We determined the effect of GTP hydrolysis inhibition on BtubA/B filament dynamics by visualizing BtubA/B polymerization in 12.5 mM KCl and in the presence of the nonhydrolyzable GTP analog, GMPCPP. We observed a large number of short filament bundles of about 10 μm in length, and between the 5- and 10-min time points bundles were not dynamic (Fig. 6A). The bidirectional polymerization of BtubA/B filaments from seeds at a low KCl concentration (Fig. 6A; see also Fig. S4E) indicates that seeds can form bundles composed of antiparallel filaments even in low salt. In most experiments, the GMPCPP-stabilized seed mixture was centrifuged to remove excess GMPCPP. The high concentration in the seed pellet may induce bundling. To reduce the formation of bundled seeds, we synthetized the seeds without centrifugation, added the seed solution directly to the reaction chamber, and washed out the GMPCPP while the seeds were attached to the surface. We then flowed in 5 μM BtubA/B in 12.5 mM KCl and 1 mM GTP. The growing filaments formed long and stable bundles without dynamic rearrangement over time (Fig. 6B; see also Movie S5 in the supplemental material). We interpret these data as evidence that trace amounts of GMPCPP (<5 μM) remaining in the reaction chamber can stabilize the filaments against breakage.

DISCUSSION

In this study, we have characterized the biochemical properties, assembly polarity, and dynamics of BtubA/B filaments. We determined that BtubA/B assembly is kinetically polar, and its assembly dynamics are affected by KCl concentration. At low KCl concentration, single BtubA/B filaments grow and shrink stochastically via fast contin-
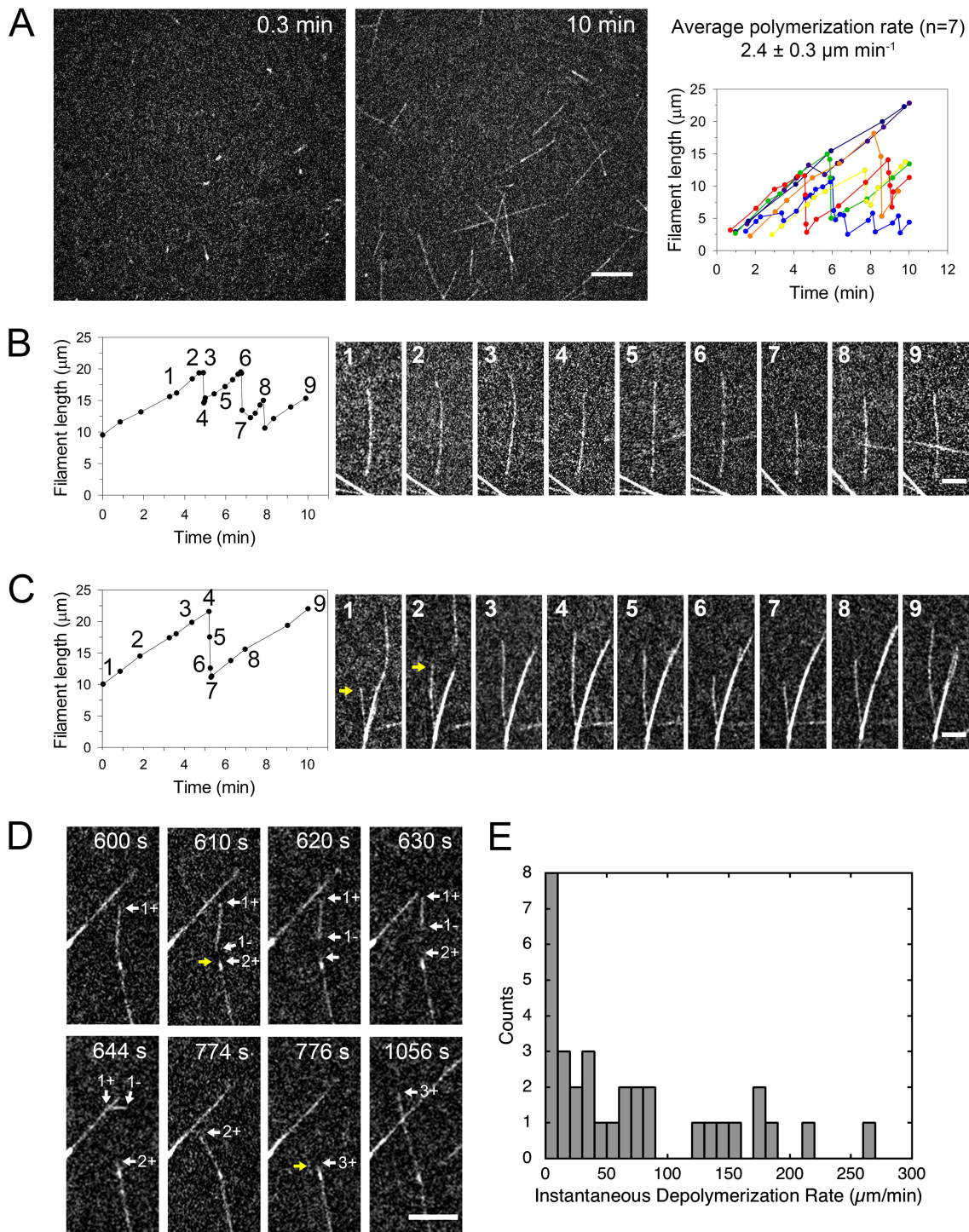
FIG 5 Visualization of BtubA/B polymerization at low KCl concentration. Bacterial BtubA/B filaments alternate between steady growth and shrinking. (A) Time-lapse images of 3 μM BtubA/B (30% TAMRA labeled) assembly from seeds in 12.5 mM KCl and 1 mM GTP. (Right) Filament length versus time for seven single filaments growing from GMPCPP-stabilized seeds. (B) Fast shortening of a single BtubA/B filament. (Left) Change in length as a function of time of the single BtubA/B filament. (Right) Dynamically unstable filament elongating from a seed at 2.2 $\pm$ 0.2 μm min^{-1}. (C) Fast continuous depolymerization of a single BtubA/B filament. (Left) Change in length as a function of time of the BtubA/B filament. Filament elongation at 2.3 $\pm$ 0.3 μm min^{-1} and continuous depolymerization of a single BtubA/B filament (arrows). (D) Spontaneous breakage (yellow arrows) of a growing filament ("1+," where "+" denotes the growing end of the filament) generates a fragment that remains bound to the surface. The new plus end ("2+") resumes growth, and the new minus end of the BtubA/B fragment ("1−," where "−" denotes the shrinking end) starts depolymerizing faster than the plus end of the fragment ("1+"). At 776 s, spontaneous breakage (yellow arrows) generates a new growing plus end ("3+"). (E) The histogram of depolymerization rates of single BtubA/B filaments shows a population of filament with an average depolymerization velocity of 33 μm min^{-1} and a higher depolymerization rate of 175 μm min^{-1}. Images were preprocessed as described in Materials and Methods. Scale bars, 10 μm (A and C) and 5 μm (B).
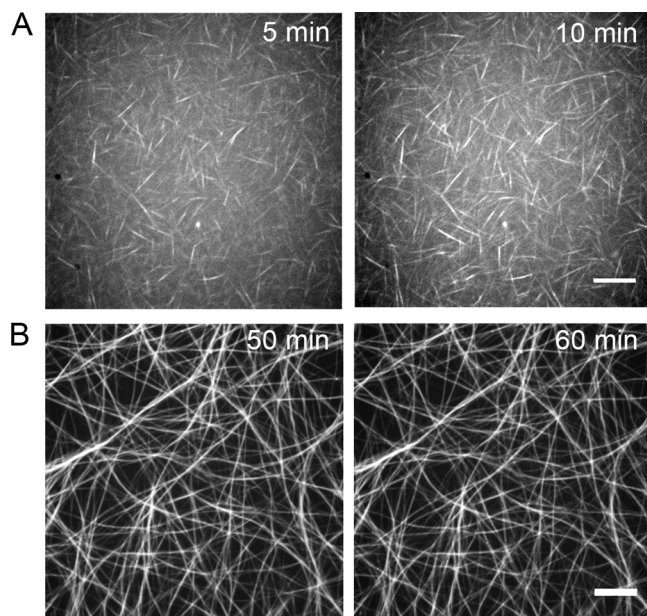
FIG 6 BtubA/B polymerization with the slowly hydrolyzable analog GMPCPP. (A) A total of 5 μM BtubA/B (30% TAMRA labeled) polymerized in the presence of 1 mM GMPCPP and 12.5 mM KCl. Seeds are brighter and denser than in polymerization with GTP (Fig. S4D), indicating that they contain several bundled filaments. (B) A total of 5 μM BtubA/B (30% TAMRA-labeled BtubA/B) polymerized in the presence of 12.5 mM KCl by adding 1 mM GTP and trace GMPCPP. BtubA/B form long and interconnected bundles that remain stable even at 60 min after GTP addition. Transitions between filament growth and fragmentation were not observed. Scale bars, 10 μm (A and B).

uous filament depolymerization, as well as possible fast fragmentation. The increase of KCl concentration reduces the critical concentration of BtubA/B assembly and induces filament bundling. Interestingly, KCl and NaCl have different effects on BtubA/B polymerization, suggesting that the interaction is not purely due to ionic strength. This observation is in keeping with other cytoskeletal polymers that have monovalent cation-specific binding sites that affect polymerization or filament stability. For example, eukaryotic actin binds twice as many K$^+$ ions as Na$^+$ ions upon polymerization (24), and the haloarchaeal tubulin FtsZ1 polymerizes *in vitro* at high K$^+$ but not at high Na$^+$ concentrations (25).

We imaged the products of BtubA/B polymerization in a range of salt conditions using both fluorescence and electron microscopy (Fig. 1). At low salt, we observed single filaments, which under negative stain appear as two light protofilaments flanking a dark center. This appearance of the BtubA/B filaments is similar to previous observations of BtubA/B polymerized *in vitro* and imaged with negative stain electron microscopy (2, 3, 5), but it may also be interpreted as the projection of the light walls of a 5-protofilament bacterial microtubule flanking a dark tubule lumen (8). Such a 5-protofilament tubule structure may have a similar overall diameter and appearance when viewed in projection as in negative stain electron microscopy, explaining the difference between *in vitro* and *in vivo* results. More work is needed with multiple modalities of electron microscopy to fully resolve this question.

Using light scattering (see Fig. S2 in the supplemental material), we determined that below 25 mM KCl, BtubA/B follow a nucleation-elongation mechanism of assembly. At 50 mM or higher KCl concentrations, BtubA/B filaments self-associate into bundles, reducing the filament depolymerization rate. Interestingly, filament stabilization by bundling appears to be principally influenced by KCl rather than by protein concentration (Fig. 2E), and this may be the mechanism by which KCl decreases the critical concentration for polymerization. However, the reduction of critical concentration at low salt where there is no bundling (Fig. 2A and C) suggests that KCl also has a stabilizing effect on the BtubA/B interaction along a single filament. KCl appears to

favor both intra- and interheterodimer interactions as suggested by the increase of the size of the BtubA/B polymerization nucleus with increasing KCl concentration (Fig. 2B). In a complementary approach, we found that the effective total GTP hydrolysis rate increases between 0 and 25 mM KCl and decreases above 50 mM KCl (Fig. 2F; see also Table S1 in the supplemental material), which is likely due to the onset of BtubA/B filament bundling (Fig. 1; see also Fig. S2F) that stabilizes the polymer and reduces the free (unpolymerized) BtubA/B heterodimer concentration. Bundling therefore appears to be an important modulator of BtubA/B filament dynamics, which may have implications for their function in either *Prosthecobacter* or in the ancient eukaryotic ancestor in which the ancestral microtubule existed.

We visualized the dynamics of fluorescently labeled BtubA/B filaments using confocal fluorescence microscopy and determined that, like eukaryotic MTs, BtubA/B polymers are kinetically polar polymers at low and intermediate salt concentrations (Fig. 3; see also Fig. S3 in the supplemental material). At the fast-growing plus end, BtubA/B polymer growth rates at 3 μM BtubA/B dimer concentration, measured at 2.4 to 3.7 μm min^{-1}, are 6- to 15-fold higher than the rates of assembly observed for eukaryotic microtubules measured at similar tubulin concentrations: 0.5 μm min^{-1} for 4.5 μM GTP-tubulin (26) and 0.1 μm min^{-1} for 1.5 μM GMPCPP-tubulin (27). In the presence of GTP, the filaments exhibit complex dynamics, including continuous treadmilling (Fig. 4D) and stochastic switching between growth and fast disassembly (Fig. 5B and C). Treadmilling has also been observed in the plasmid-encoded bacterial tubulin TubZ (28, 29), FtsZ filaments (30, 31), as well as in eukaryotic MTs. BtubA/B filament treadmilling indicates that GDP/GTP exchange can only occur in the free heterodimers because it occurs when monomers at the plus end are GTP bound and monomers at the minus end are GDP bound. Such a hydrolysis state gradient is inconsistent with exchange in the filament wall. The stochastic switching between growth and disassembly is similar to the dynamic instability seen in eukaryotic MTs as well as in filaments formed by the distantly related bacteriophage phage tubulin PhuZ (32) and the actin-related protein ParM (18, 22). These dynamic behaviors are suppressed by the slowly hydrolyzable GTP analogue GMPCPP (Fig. 6), indicating that GTP hydrolysis is necessary for BtubA/B filament destabilization and disassembly as for eukaryotic MTs.

In eukaryotic MTs, loss of the stabilizing cap of GTP-bound monomers at the plus end leads to filament depolymerization and the gain of a GTP cap rescues polymerization (11–13). With the imaging modality and fluorescent labeling used in this study, it is difficult to observe the fast continuous depolymerization, which would unequivocally confirm BtubA/B dynamic instability, but we were able to track the ends of some filaments during the shortening phase in frames in which the ends were in focus. Our results are consistent with a range of disassembly rates that can be classified into low rates with an average of 32 μm min^{-1}, which is comparable to the rate of 28 μm min^{-1} observed for eukaryotic microtubules (26), and high disassembly rates with an average of 175 μm min^{-1}. It is possible that BtubA/B filament disassembly occurs due to a GTP hydrolysis-induced loss of filament stability that leads to catastrophic fragmentation of the filament via multiple breaks into filaments that diffuse away too quickly to observe, and this may explain the high disassembly rates that we occasionally observe. We have observed rescue of polymerization after filament breakage into larger pieces (Fig. 5B) as well as short depolymerization events. The lower number of protofilaments in BtubA/B filaments may render them more prone to fragmentation than eukaryotic MTs. Fast disassembly may then occur as a combination of fragmentation and fast depolymerization at the new plus end. We conclude that at low KCl concentration, single BtubA/B filaments are dynamic filaments with transitions between steady growth and disassembly, consisting of fast filament depolymerization and/or fragmentation, processes that are modulated by GTP hydrolysis state.

Our experiments in a range of buffer conditions show that BtubA/B filaments differ from eukaryotic MTs in their strong tendency to assemble into irregular and apolar bundles in high salt concentrations. Bundling does not require any other proteins. Preexisting single filaments can zipper together into bundles and keep growing (Fig. 4B

and C). BtubA/B filaments stabilized by GMPCPP were observed to bundle even in low salt (12.5 mM KCl) (Fig. 6), possibly due to the sum of many weak interactions along their lengths. An attractive but nonstereospecific interaction, such as a hydrophobic interaction or van der Waals forces between filaments may be responsible for the bundling, and for short filaments, salt is needed to screen the charge on filaments. Crowding agents also enhance BtubA/B polymerization and induce the bundling of BtubA/B filaments (5). We did not observe breakage of bundled filaments, suggesting that bundling mechanically stabilizes them. Although this bundling may not fully recapitulate the filament bundling that occurs *in vivo* due to the action of additional BtubA/B interacting proteins in the bacterial cytoplasm, it is an unusual behavior that is interesting in the context of understanding how sequence variation in the tubulin family leads to a variety of biophysical properties.

The function of BtubA/B filaments *in vivo* is still unknown. In *Prosthecobacter*, single filaments of 0.2 to 1.2 μm in length, or bundles composed of 2, 3, or 4 filaments, are located in or near the base of the cellular extension called prostheca (8). BtubA/B filaments or their bundles may support the elongated shape of the prostheca (2, 5), but so far, evidence suggests that BtubA/B filaments are not determinants of the *Prosthecobacter* cell morphology because at least one *Prosthecobacter* species without *btubA* and *btubB* genes maintains the prosthecate morphology (33). It may be that these filaments play a nonessential stabilizing role or an intracellular transport role that increases the efficiency or robustness of prostheca formation and maintenance in most *Prosthecobacter* species. BtubA/B filaments that we observed using EM at high salt (Fig. 1B) appear to be more tightly BtubA/B bundled than those observed in *Prosthecobacter* (8), but bundles of several filaments are visible in the cells, suggesting that the bundled form may be functionally relevant. The difference in the tightness of the bundle may be attributed to the protein Bklc of the *btub* operon, which is expressed in *Prosthecobacter* and has been shown to interact with both BtubA/B filaments and lipid membranes *in vitro* (9). Although *in vitro*, Bklc does not change the bundling of BtubA/B polymers (9), *in vivo*, looser bundling may occur as a consequence of association with the cell membrane. Due to the lack of genetics tools in *Prosthecobacter*, the controlled expression and visualization of fluorescently tagged BtubA/B in *Escherichia coli* would be useful for determining the dynamics and function of BtubA/B filaments in a cell environment. Ultimately, BtubA/B filament function in *Prosthecobacter* will also need to be understood in the context of polymerized BtubA/B-binding proteins that potentially regulate their dynamics *in vivo*. Interestingly, although the protein product of the *bklc* gene binds BtubA/B polymers, it does not appear to affect the dynamic parameters of these polymers (9).

In addition to their unknown function in *Prosthecobacter*, BtubA/B filaments are of ultimate interest as an evolutionary link between eukaryotic microtubules and the ancient microtubule from which the BtubA/B genes are derived. BtubA/B have more sequence and structure in common with eukaryotic tubulins than any other bacterial tubulin, and the presence of both *btubA* and *btubB* genes suggests that the horizontal transfer event that is thought to have occurred not long after the initial duplication event created the ancestors of the A and B and α and β homolog pairs (7). The more evolutionarily distant phage tubulin PhuZ has been demonstrated to exhibit dynamic instability (32) and to segregate DNA (34). We cannot exclude the possibility that filament dynamics evolved after the horizontal gene transfer to *Prosthecobacter* and that any similarities between the dynamics of BtubA/B filaments, phage tubulin filaments, and eukaryotic MTs are the result of convergent evolution. In either situation, however, BtubA/B provide a simple model of bacterially expressed tubulins that can be used to study the structural determinants of microtubule dynamics.

Further work on the structural changes in the BtubA/B dimer in response to GTP hydrolysis and polymerization, as well as *in vivo* characterization of Bklc will illuminate the extent to which BtubA/B and the ancient tubulin ancestor may have functioned in DNA segregation or other cellular functions.

MATERIALS AND METHODS

BtubA/B purification. A vector containing the *Prosthecobacter dejongeii btubA* and *btubB* genes under the control of a T7 promoter (kindly provided by D. Schlieper and J. Löwe) was transformed into *E. coli* BL21(DE3) cells. A single *E. coli* BL21(DE3) colony was grown at 37°C to an optical density of 0.6 at 600 nm, and BtubA/B overexpression was induced by adding 0.3 mM isopropyl-β-D-thioga-lactopyranoside (IPTG) to the cell culture. After 4 h, the cell culture was centrifuged at 5,000 × g for 35 min, and the cell pellet was suspended with ice-cold TEN buffer (50 mM Tris-HCl [pH 8], 1 mM EDTA, 100 mM NaCl). This procedure was repeated twice to wash away LB medium and then was repeated 2 times using 50 mM HEPES-KOH (pH 7) buffer. The cell pellet was frozen at −80°C for later use. The pellet was thawed on ice and suspended in 4 volumes of cold 50 mM HEPES-KOH (pH 7) and 1 mM phenylmeth-ylsulfonyl fluoride (PMSF). The suspension mixture was sonicated on ice seven times with 20-s bursts at 7.0 W with a Misonix 3000 sonicator. The lysate was centrifuged at 100,000 × g for 1 h at 4°C, the supernatant was recovered, and the pellet was discarded. The supernatant was warmed to 25°C, its volume was measured, and 5 mM MgCl$_2$ (2 M stock solution) and 0.5 M KCl (solid to minimize the increase in volume) were added. The solution was mixed gently, and it was incubated at 25°C for 10 min. The first BtubA/B polymerization/depolymerization cycle was started by adding 2 mM GTP. The solution was gently mixed and centrifuged immediately at 100,000 × g for 30 min at 25°C. The supernatant was discarded, and the pellet was solubilized by pipetting with 3 to 4 volumes of ice-cold 50 mM HEPES-KOH (pH 7) buffer. It was then incubated in ice for 30 min (low temperature reduces BtubA/B polymerization as with eukaryotic MTs), with occasional pipetting, and was ultracentrifuged at 100,000 × g for 30 min at 4°C. The pellet was discarded. This completed one polymerization/depolymerization cycle. The supernatant was warmed again at 25°C, and a total of three cycles of polymerization/depolymerization were completed using the same conditions. The last solubilized pellet was dialyzed twice against 1,000 volumes of 50 mM HEPES-KOH (pH 7) buffer, then the protein solution was ultracentrifuged at 100,000 × g for 15 min at 4°C to remove aggregates, and the protein in the supernatant was stored in aliquots at −80°C.

Quantification of BtubA/B concentration. BtubA/B batch stock concentration was determined by the bicinchoninic acid (BCA) assay and using BtubA/B of known concentration as a standard. BtubA/B standard concentration was quantified by measuring its absorbance at 280 nm after nucleotide exchange; an aliquot of BtubA/B was incubated with 2 mM GTP and 5 mM MgCl$_2$ for 1 h in ice to exchange any GDP bound to BtubA/B. The free nucleotide was removed using a Bio-Gel P-6 polyacrylamide gel chromatography column (Bio-Rad), previously equilibrated with polymerization buffer (50 mM HEPES-KOH [pH 7], 5 mM MgCl$_2$). The eluent was ultracentrifuged at 100,000 × g for 15 min at 4°C to remove aggregates and BtubA/B polymers. A 1:100 dilution of the supernatant (BtubA/B bound to GTP) in polymerization buffer was performed to measure its absorbance at 280 nm using an extinction coefficient of 103,754.2 M^{-1} cm^{-1} (BtubA, 47,900 M^{-1} cm^{-1}; BtubB, 39,880 M^{-1} cm^{-1}; 2 GTPs, 7,987.1 M^{-1} cm^{-1} each). For the light scattering, high-speed pelleting, and GTP hydrolysis assays, 20 μM BtubA/B in different KCl polymerization buffers was prepared from 400 μM BtubA/B stock, resulting in a KCl and MgCl$_2$ concentration decrease of 5% from the nominal value. The 20 μM BtubA/B solution was serially diluted in 0.75-fold increments (20, 15, 11.3, 8.4, 6.3, 4.8, 3.6, 2.7, 2, and 1.5 μM BtubA/B) using the same KCl polymerization buffer.

Fluorescent labeling of BtubA/B. A total of 200 μM BtubA/B in 50 mM HEPES (pH 7) was fluorescently labeled by adding a 10-fold molar excess of TAMRA (5 [and 6]-carboxytetramethyl-rhodamine, succinimidyl ester, mixed isomers; Molecular Probes) or Alexa Fluor 488 (Molecular Probes) for 1 h on ice with occasional stirring. Labeled BtubA/B were separated from the free dye by Bio-Gel P-6 polyacrylamide gel chromatography columns (Bio-Rad). Labeled BtubA/B were warmed to room temperature, and 200 mM KCl and 5 mM MgCl$_2$ were added to it. Labeled and functional BtubA/B were selected by the addition of 1 mM GTP, and the solution was immediately centrifuged at 100,000 × g for 15 min at 25°C. The pellet was suspended in 50 mM HEPES-KOH (pH 7) and centrifuged at 100,000 × g for 15 min at 4°C. The supernatant was dialyzed against 50 mM HEPES-KOH (pH 7) for 4 h and then was stored in aliquots at −80°C. Final labeling stoichiometry was 1 to 2 dyes per BtubA/B heterodimer.

Electron microscopy. A total of 5 μM BtubA/B in polymerization buffer (50 mM HEPES-KOH [pH 7], 5 mM MgCl$_2$) with different KCl concentrations was polymerized by adding 1 mM GTP at 25°C. After 5 min, 4 μl of the reaction mixture was transferred to glow-discharged 200-mesh carbon Formvar-coated copper grids at 25°C. The grids were washed with three drops of the same KCl polymerization buffer and were negatively stained with 0.75% uranyl formate. The sample images were obtained at 25°C with a Tecnai T12 microscope using an acceleration voltage of 120 kV and a magnification of ×52,000. Images were recorded with a Gatan 4k × 4k charge-coupled-device (CCD) camera.

Light scattering. BtubA/B polymerization kinetics was measured by 90° light scattering on a PerkinElmer spectrofluorimeter LS-50B using an excitation and emission wavelength of 350 nm, 5 nm excitation and emission bandwidths, and a transmission filter of 4%. Each BtubA/B solution was loaded in a quartz cuvette with a 1-cm path length, and the light scattering of the solution was measured for 5 min at 25°C to establish the baseline. Polymerization was initiated by adding 1 mM GTP to the cuvette, which was gently homogenized by inversion (3 times). The light scattering intensity was measured starting 15 s after the addition of nucleotide. The steady-state BtubA/B concentration was determined from the difference between the maximum intensity value and the average intensity of the 5-min baseline of each kinetic trace. This net intensity was plotted as a function of the initial BtubA/B concentration. The x axis intercept of the linear fit to the plot corresponds to the critical concentration of unpolymerized BtubA/B.

High-speed pelleting. For the pelleting assays, reactions started by adding 1 mM GTP to the BtubA/B solutions and were immediately centrifuged at 100,000 × *g* in a TLA-100.4 rotor for 15 min at 25°C. Precipitates were suspended in the starting volume of the reaction mixture without KCl in the polymerization buffer, and BtubA/B were quantified by the BCA assay using the serial dilution of BtubA/B as a calibration curve. The critical concentration for the BtubA/B assembly was determined by plotting BtubA/B in the pellet as a function of the initial BtubA/B concentration. The *x* axis intercept of the linear fit to the plot corresponds to the steady-state concentration of unpolymerized BtubA/B.

GTP hydrolysis assay. GTPase activity (phosphate release [P_i]) was measured by the malachite green colorimetric assay (35). The reaction was started by adding 1 mM GTP to the BtubA/B solutions. At 0 and 5 min, 50-μl aliquots were added to tubes containing 350 μl of Nanopure water and 400 μl of perchloric acid, mixed and placed in ice to stop GTP hydrolysis. After 30 min, 200 μl of the dye solution was added to the 800-μl sample, the sample was incubated for 10 min at 25°C, and absorbance was measured at 630 nm. The standard curve was constructed with monobasic potassium phosphate dissolved in Nanopure water and had a linear range between 0.5 and 10 nmol of inorganic phosphate. The rate of GTP hydrolysis (P_i [micromolar] per minute) was calculated from the difference between the measurement at 5 min and time zero. We plotted the rates of GTP hydrolysis as a function of BtubA/B concentration. The slope of the line fit corresponds to BtubA/B GTPase activity.

Kinetic polarity assay of BtubA/B assembly. A total of 20 μl of 5 μM BtubA/B (30% TAMRA labeled) was assembled by the addition of 0.5 mM GMPCPP (50 mM HEPES-KOH [pH 7], 5 mM MgCl$_2$, 0 to 500 mM KCl). After 2 min, 20 μl of 5 μM BtubA/B labeled with Alexa Fluor 488 (30% Alexa Fluor 488 labeled) was added to the reaction mixture. After 2 min, 1 μl of the reaction mixture was diluted in 200 μl of polymerization buffer and 4 μl of the dilution was added to a poly-L-lysine-coated coverslip and visualized by confocal microscopy.

Confocal microscopy. For confocal microscopy visualization of in bulk BtubA/B assembly, 5 μM BtubA/B (15% TAMRA labeled) in polymerization buffer (50 mM HEPES-KOH [pH 7], 5 mM MgCl$_2$) with different KCl concentrations (50, 100, and 1,000 mM KCl) was polymerized by adding 1 mM GTP. After 5 min, the solutions were transferred to acid-washed and poly-L-lysine-coated coverslips before visualization. Individual BtubA/B filaments growing from seeds were visualized by confocal microscopy in flow chambers made of acid-washed coverslips. Coverslips were kept overnight in 1 M HCl at 60°C, and then sonicated for 30 min in MilliQ (Millipore) distilled deionized water (twice) and in a ramp of 50%, 75%, and 95% ethanol washes. They were then stored in 95% ethanol. Coverslips were rinsed thoroughly with MilliQ water and dried with a nitrogen stream before use. The assembly assay was adapted from the method described by Brouhard et al. (36) with minor modifications. Flow chambers were incubated with antirhodamine antibody (Invitrogen) diluted 1:100 in polymerization buffer at room temperature for 15 min. The flow chamber was washed with polymerization buffer followed by two washes of blocking solution (1% pluronic acid 127 [Sigma] in polymerization buffer) for 10 min. BtubA/B seeds diluted 1:100 in blocking buffer were added to the flow chambers and were incubated for 5 min at room temperature. The flow channels were washed with blocking buffer, and the BtubA/B assembly reaction was added to the flow channels. The BtubA/B assembly reaction was supplemented with a glucose oxidase oxygen scavenger system consisting of 250 μg/ml glucose oxidase (Sigma-Aldrich), 4.5 mg/ml glucose, and 30 μg/ml catalase (Roche). The BtubA/B seeds were synthetized by polymerizing 5 μM BtubA/B (40% TAMRA labeled) in polymerization buffer with 12.5 or 100 mM KCl by adding 0.5 mM GMPCPP for 5 min at room temperature. The solution was centrifuged at 100,000 × *g* for 15 min, the supernatant was discarded, and the pellet was suspended in polymerization buffer, followed by a second centrifugation and suspension in polymerization buffer. Samples were imaged with a Carl Zeiss (Oberkochen, Germany) Axio Observer Z1 inverted microscope with a Zeiss ×63, 1.4-numerical-aperture Plan Apochromat oil immersion objective, a Yokogawa (Sugar Land, TX) CSU 10 confocal scanner unit, and a Photometrics (Tucson, AZ) Cascade II 512 CCD camera. For confocal illumination, Cobolt (Stockholm, Sweden) Calypso 491-nm and Jive 561-nm lasers were used with a laser launch built by Solamere Technology group (Salt Lake City, UT). Images were acquired with Molecular Devices (Sunnyvale, CA) MetaMorph software. The pixel calibration was 165 nm/pixel or 103 nm/pixel, controlled by a tube lens that provided ×1 or ×1.6 additional magnification. Images were preprocessed by subtraction of a background approximated by the rolling ball algorithm with a diameter of 10 pixels. All image processing and analysis was performed using ImageJ.

SUPPLEMENTAL MATERIAL

Supplemental material for this article may be found at https://doi.org/10.1128/JB.00211-17.

SUPPLEMENTAL FILE 1, PDF file, 1.2 MB.
SUPPLEMENTAL FILE 2, AVI file, 19.2 MB.
SUPPLEMENTAL FILE 3, AVI file, 18.9 MB.
SUPPLEMENTAL FILE 4, AVI file, 10.7 MB.
SUPPLEMENTAL FILE 5, AVI file, 16.1 MB.
SUPPLEMENTAL FILE 6, AVI file, 11.7 MB.

ACKNOWLEDGMENTS

REFERENCES

1. Jenkins C, Samudrala R, Anderson I, Hedlund BP, Petroni G, Michailova N, Pinel N, Overbeek R, Rosati G, Staley JT. 2002. Genes for the cytoskeletal protein tubulin in the bacterial genus *Prosthecobacter*. Proc Natl Acad Sci U S A 99:17049–17054. https://doi.org/10.1073/pnas.012516899.

2. Sontag CA, Staley JT, Erickson HP. 2005. *In vitro* assembly and GTP hydrolysis by bacterial tubulins BtubA and BtubB. J Cell Biol 169:233–238. https://doi.org/10.1083/jcb.200410027.

3. Schlieper D, Oliva MA, Andreu JM, Lowe J. 2005. Structure of bacterial tubulin BtubA/B: evidence for horizontal gene transfer. Proc Natl Acad Sci U S A 102:9170–9175. https://doi.org/10.1073/pnas.0502859102.

4. Pilhofer M, Bauer AP, Schrallhammer M, Richter L, Ludwig W, Schleifer KH, Petroni G. 2007. Characterization of bacterial operons consisting of two tubulins and a kinesin-like gene by the novel two-step gene walking method. Nucleic Acids Res 35:e135. https://doi.org/10.1093/nar/gkm836.

5. Martin-Galiano AJ, Oliva MA, Sanz L, Bhattacharyya A, Serna M, Yebenes H, Valpuesta JM, Andreu JM. 2011. Bacterial tubulin distinct loop sequences and primitive assembly properties support its origin from a eukaryotic tubulin ancestor. J Biol Chem 286:19789–19803. https://doi.org/10.1074/jbc.M111.230094.

6. Pilhofer M, Rosati G, Ludwig W, Schleifer KH, Petroni G. 2007. Coexistence of tubulins and ftsZ in different *Prosthecobacter* species. Mol Biol Evol 24:1439–1442. https://doi.org/10.1093/molbev/msm069.

7. Findeisen P, Muhlhausen S, Dempewolf S, Hertzog J, Zietlow A, Carlomagno T, Kollmar M. 2014. Six subgroups and extensive recent duplications characterize the evolution of the eukaryotic tubulin protein family. Genome Biol Evol 6:2274–2288. https://doi.org/10.1093/gbe/evu187.

8. Pilhofer M, Ladinsky MS, McDowall AW, Petroni G, Jensen GJ. 2011. Microtubules in bacteria: ancient tubulins build a five-protofilament homolog of the eukaryotic cytoskeleton. PLoS Biol 9:e1001213. https://doi.org/10.1371/journal.pbio.1001213.

9. Akendengue L, Trepout S, Grana M, Voegele A, Janke C, Raynal B, Chenal A, Marco S, Wehenkel AM. 2017. Bacterial kinesin light chain (Bklc) links the Btub cytoskeleton to membranes. Sci Rep 7:45668. https://doi.org/10.1038/srep45668.

10. Sontag CA, Sage H, Erickson HP. 2009. BtubA-BtubB heterodimer is an essential intermediate in protofilament assembly. PLoS One 4:e7253. https://doi.org/10.1371/journal.pone.0007253.

11. Desai A, Mitchison TJ. 1997. Microtubule polymerization dynamics. Annu Rev Cell Dev Biol 13:83–117. https://doi.org/10.1146/annurev.cellbio.13.1.83.

12. Howard J, Hyman AA. 2003. Dynamics and mechanics of the microtubule plus end. Nature 422:753–758. https://doi.org/10.1038/nature01600.

13. Erickson HP, O'Brien ET. 1992. Microtubule dynamic instability and GTP hydrolysis. Annu Rev Biophys Biomol Struct 21:145–166. https://doi.org/10.1146/annurev.bb.21.060192.001045.

14. Haeusser DP, Margolin W. 2012. Bacteriophage tubulins: carrying their own cytoskeleton key. Curr Biol 22:R639–R641. https://doi.org/10.1016/j.cub.2012.07.027.

15. Löwe J, Amos LA. 2009. Evolution of cytomotive filaments: the cytoskeleton from prokaryotes to eukaryotes. Int J Biochem Cell Biol 41:323–329. https://doi.org/10.1016/j.biocel.2008.08.010.

16. Mitchison T, Kirschner M. 1984. Dynamic instability of microtubule growth. Nature 312:237–242. https://doi.org/10.1038/312237a0.

17. Tobacman LS, Korn ED. 1982. The regulation of actin polymerization and the inhibition of monomeric actin ATPase activity by *Acanthamoeba* profilin. J Biol Chem 257:4166–4170.

18. Rivera CR, Kollman JM, Polka JK, Agard DA, Mullins RD. 2011. Architecture and assembly of a divergent member of the ParM family of bacterial actin-like proteins. J Biol Chem 286:14282–14290. https://doi.org/10.1074/jbc.M110.203828.

19. Nishida E, Sakai H. 1983. Kinetic analysis of actin polymerization. J Biochem 93:1011–1020. https://doi.org/10.1093/oxfordjournals.jbchem.a134224.

20. Polka JK, Kollman JM, Agard DA, Mullins RD. 2009. The structure and assembly dynamics of plasmid actin AlfA imply a novel mechanism of DNA segregation. J Bacteriol 191:6219–6230. https://doi.org/10.1128/JB.00676-09.

21. van den Ent F, Moller-Jensen J, Amos LA, Gerdes K, Lowe J. 2002. F-actin-like filaments formed by plasmid segregation protein ParM. EMBO J 21:6935–6943. https://doi.org/10.1093/emboj/cdf672.

22. Garner EC, Campbell CS, Mullins RD. 2004. Dynamic instability in a DNA-segregating prokaryotic actin homolog. Science 306:1021–1025. https://doi.org/10.1126/science.1101313.

23. Gayathri P, Fujii T, Moller-Jensen J, van den Ent F, Namba K, Lowe J. 2012. A bipolar spindle of antiparallel ParM filaments drives bacterial plasmid segregation. Science 338:1334–1337. https://doi.org/10.1126/science.1229091.

24. Kang H, Bradley MJ, McCullough BR, Pierre A, Grintsevich EE, Reisler E, De La Cruz EM. 2012. Identification of cation-binding sites on actin that drive polymerization and modulate bending stiffness. Proc Natl Acad Sci U S A 109:16923–16927. https://doi.org/10.1073/pnas.1211078109.

25. Ozawa K, Harashina T, Yatsunami R, Nakamura S. 2005. Gene cloning, expression and partial characterization of cell division protein FtsZ1 from extremely halophilic archaeon *Haloarcula japonica* strain TR-1. Extremophiles 9:281–288. https://doi.org/10.1007/s00792-005-0443-6.

26. Chretien D, Fuller SD, Karsenti E. 1995. Structure of growing microtubule ends: two-dimensional sheets close into tubes at variable rates. J Cell Biol 129:1311–1328. https://doi.org/10.1083/jcb.129.5.1311.

27. Gardner MK, Charlebois BD, Janosi IM, Howard J, Hunt AJ, Odde DJ. 2011. Rapid microtubule self-assembly kinetics. Cell 146:582–592. https://doi.org/10.1016/j.cell.2011.06.053.

28. Larsen RA, Cusumano C, Fujioka A, Lim-Fong G, Patterson P, Pogliano J. 2007. Treadmilling of a prokaryotic tubulin-like protein, TubZ, required for plasmid stability in *Bacillus thuringiensis*. Genes Dev 21:1340–1352. https://doi.org/10.1101/gad.1546107.

29. Fink G, Lowe J. 2015. Reconstitution of a prokaryotic minus end-tracking system using TubRC centromeric complexes and tubulin-like protein

TubZ filaments. Proc Natl Acad Sci U S A 112:E1845–E1850. https://doi.org/10.1073/pnas.1423746112.

30. Loose M, Mitchison TJ. 2014. The bacterial cell division proteins FtsA and FtsZ self-organize into dynamic cytoskeletal patterns. Nat Cell Biol 16:38–46. https://doi.org/10.1038/ncb2885.

31. Yang X, Lyu Z, Miguel A, McQuillen R, Huang KC, Xiao J. 2017. GTPase activity-coupled treadmilling of the bacterial tubulin FtsZ organizes septal cell wall synthesis. Science 355:744–747. https://doi.org/10.1126/science.aak9995.

32. Erb ML, Kraemer JA, Coker JK, Chaikeeratisak V, Nonejuie P, Agard DA, Pogliano J. 2014. A bacteriophage tubulin harnesses dynamic instability to center DNA in infected cells. eLife 3:e03197.

33. Takeda M, Yoneya A, Miyazaki Y, Kondo K, Makita H, Kondoh M, Suzuki I, Koizumi J. 2008. *Prosthecobacter fluviatilis* sp. nov., which lacks the bacterial tubulin *btubA* and *btubB* genes. Int J Syst Evol Microbiol 58:1561–1565. https://doi.org/10.1099/ijs.0.65787-0.

34. Kraemer JA, Erb ML, Waddling CA, Montabana EA, Zehr EA, Wang H, Nguyen K, Pham DS, Agard DA, Pogliano J. 2012. A phage tubulin assembles dynamic filaments by an atypical mechanism to center viral DNA within the host cell. Cell 149:1488–1499. https://doi.org/10.1016/j.cell.2012.04.034.

35. Geladopoulos TP, Sotiroudis TG, Evangelopoulos AE. 1991. A malachite green colorimetric assay for protein phosphatase activity. Anal Biochem 192:112–116. https://doi.org/10.1016/0003-2697(91)90194-X.

36. Brouhard GJ, Stear JH, Noetzel TL, Al-Bassam J, Kinoshita K, Harrison SC, Howard J, Hyman AA. 2008. XMAP215 is a processive microtubule polymerase. Cell 132:79–88. https://doi.org/10.1016/j.cell.2007.11.043.